Coupled Electromagnetic and Heat Transfer Model for Grain Seeds Drying in a Hybrid Dryer

Petru-Marian Cârlescu [1], Ioan Țenu [1], Marius Băetu [1], Vlad Arsenoaia [1] and Radu Roșca [1]

[1] *University of Life Sciences, 3 Mihail Sadoveanu Alley, Iași, 700490, Romania*

Abstract

A multiphysics model that coupled electric fields and heat transfer was developed to simulate microwave heating of maize seeds in a dryer. The hybrid dryer with the maize seeds inside was simulated using COMSOL Multiphysics software. The dryer was equipped with three magnetrons, with a power of 800 W each, operating at a frequency of 2.45 GHz. These magnetrons create an electric field that is absorbed by the heating maize seeds. In order to increase the accuracy of the results, a study regarding the independence of the discretization grid in the field of the dryer calculation was performed. By the action of the electric field in the dryer, the temperature in the seed layer is evenly distributed, with a maximum value of 44°C after a period of 9-12 seconds. By losing moisture, the seeds become lighter, being transported around the top of the seed layer, and are discharged from the dryer every 3-4 seconds when the feed rate of maize seed is 500 kg/h. The spiral movement of the seeds in the first half of the dryer in the regions where the distribution of the electric field that alternates from maximum to minimum, makes the temperature of the seeds to be uniform in the whole volume, achieving a uniform drying.

Keywords

hybrid dryer, microwave drying, heat transfer

1. Introduction

Seeds drying is a method of preservation that prevents microbial growth, increasing their shelf life. Drying is a complex interaction of heat, mass and impulse transport, which requires time and energy consumption. Different types of drying equipment are currently available, based on combinations of different drying techniques. This is advantageous since it uses the best of different methods to achieve more efficient drying [1, 2, 3, 4, 5]. Microwaves have been widely used to dehydrate food and other materials with humidity [6, 7, 8, 9]. Microwave heating results from volumetric heating and rapid internal vaporization of liquid water that promotes faster drying. The process does not require long heating times and therefore results in a significant reduction in drying time (10 to 75%) and increased drying rates - 4-8 times compared to pure convective drying [10, 11, 12, 13]. Microwave drying characteristics are different for different sizes and shapes of the same product [14, 15]. The use of Lambert's law was the norm to qualitatively explain the penetration of microwaves into materials [16].

The temperature distribution of materials of different shapes during microwave heating was measured experimentally by mapping, and uneven heating was found to occur [17]. In order to address the unevenness of heating products, two techniques were commonly used: microwave output power control and power cycle [18]. In this study, for the drying process, a heat transfer model was coupled with an electromagnetic one into a hybrid dryer, in order to improve the drying uniformity in the seed layer in a short time.

Proceedings of HAICTA 2022, September 22–25, 2022, Athens, Greece
EMAIL: pcarlescu@uaiasi.ro (A. 1); itenu@uaiasi.ro (A. 2); mbaetu@uaiasi.ro (A. 3); vnarsenoaia@uaiasi.ro (A. 4); rrosca@uaiasi.ro (A. 5)
ORCID: 0000-0003-1039-0412 (A. 1); 0000-0001-5633-522X (A. 2); 0000-0003-4222-2165 (A. 5)


2. Materials and Methods

In this study, a multiphysics simulation of a hybrid dryer was performed using a heat transfer model and an electromagnetic one. The geometric model of the dryer, the properties of the material, the equations governing the models, the initial and boundary conditions are briefly described in the following sections.

2.1. Multiphysics Simulation

2.1.1. Geometry

The geometry of the hybrid dryer, the seed layer to be dried, as well as the positioning of the waveguides on the dryer must be accurately described, so as not to affect the accuracy of the distribution of the electric field inside the created cavity. Any protrusion or cavity in the wall of the dryer, as well as the angles made by the walls can substantially change the distribution of the electric field inside, Figure 1. The geometric model used in the simulation must be accurate for a more accurate representation of the electric field distribution and the temperature in the dryer.

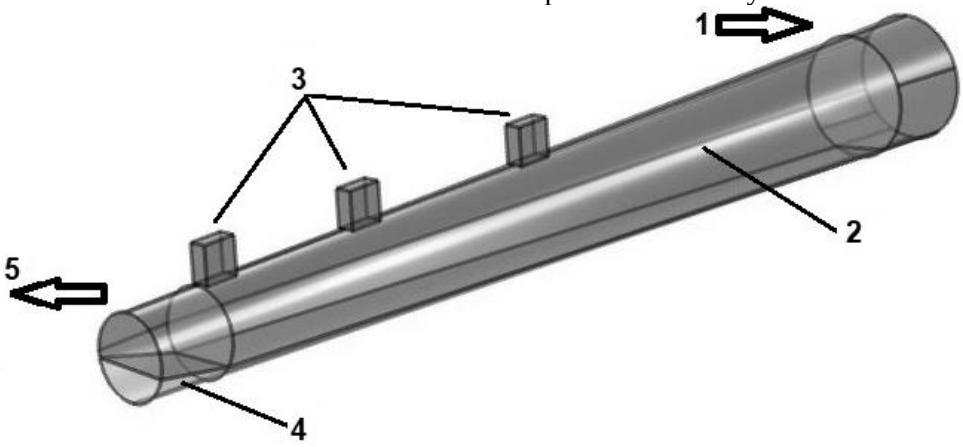

Figure 1: Truncated cone geometry of the hybrid dryer. 1 input - wet seeds and warm air; 2 truncated cone dryer; 3 waveguides with magnetrons; 4 seeds subjected to drying; 5 output -seed dryer.

The dimensions of the hybrid dryer used in the simulation are presented in Table 1.

Table 1

Dimensions of the hybrid dryer

Elements	Units (m)
Dryer length	2.5
Large diameter dryer	0.45
Small diameter dryer	0.30
Input size (air-seeds) mixture	0.2x0.1
Output size (air-seeds) mixture	0.2x0.1

In this geometric model the electromagnetic waves generated by the magnetron enter the dryer cavity through three parallelepipedic waveguides of 2 wavelengths = 244.9 mm (attributing in COMSOL Multiphysics 5.6 [19] the model TE10), located on the upper generator of the dryer. The frequency of the microwaves generated by each magnetron was 2.45 GHz and the nominal microwave power was 800 W.

2.1.2. Mesh Size

Solving electromagnetic and heat transfer models required the discretization of the entire dryer in small volumes. Thus, an appropriate mesh size in the model simulation can provide accurate simulation

results, with higher computation efficiency. The space discretization errors could be reduced to a quarter when mesh size is halved, while the computation time will increase by almost 16 times [20]. To determine the appropriate mesh size in our model, normalized power absorption (NPA) of the processing materials has been employed to complete the mesh independent study [21]. Here, the variation of NPA with mesh sizes is shown in Figure 2.

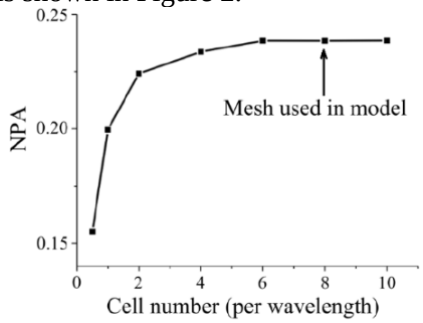

Figure 2: Normalized power absorption (NPA) variation of heating computations with different mesh sizes

The manual of software QuickWave (QWED, Warsaw, Poland) suggests the use of 12 cells per wavelength for mesh independent results, while other researchers [22] suggest that 10 cells per wavelength would be enough. The mesh size used in this paper is defined as:

$$m_{meshsize} \leq \frac{c}{6f\sqrt{\varepsilon_r}}, \quad (1)$$

where c is the speed of light, f is the frequency, ε_r is the relative permittivity.

The discretization in the air region of the dryer was based on 8 cells, compared to the region where the seeds are located where 10 cells were (Figure 3).

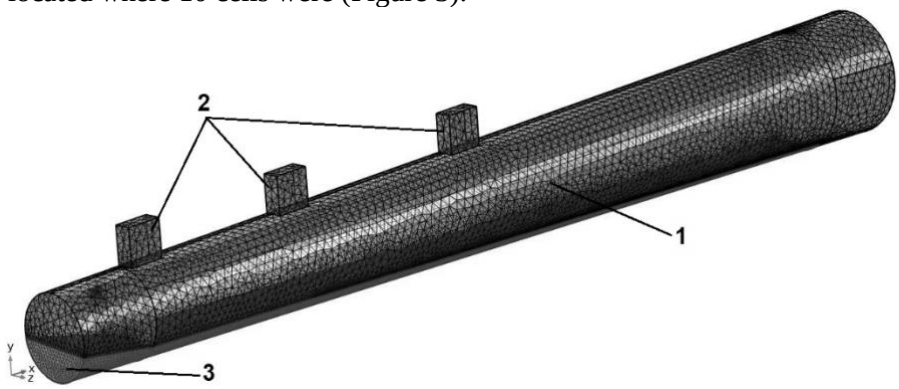

Figure 3: The space discretization of dryer geometry. 1 truncated cone dryer; 2 waveguides with magnetrons; 3 seeds subjected to drying

2.1.3. The Physical Model

The model applied in the microwave-heat transfer coupled simulation was based on the following hypotheses: the geometry and volume of the seeds do not change during the simulation; the initial temperature distribution is uniform in the seed; the thermal and dielectric properties of the maize seeds are temperature dependent; density was considered at the seed (particle) level and does not vary over time; uniform heat transfer through conduction between seeds; negligible heat transfer between the walls of the dryer and the air inside the dryer.

The whole simulation combines two physical processes: the microwave propagation process and the heat transfer in solid.

The electromagnetic waves generated inside the dryer cavity are reflected multiple times by the metal walls of the dryer, forming models of stationary electromagnetic field in the dryer.

The electric field intensity $\vec{E}$, a vector quantity, at any point in the calculation range in the dryer was calculated from Maxwell's equations [23]. The combined waveform of Maxwell's equations is expressed by the equation:

$$\nabla \times \mu_r^{-1}(\nabla \times \vec{E}) - \left(\omega\sqrt{\varepsilon_0\mu_0}\right)^2\left(\varepsilon_r\varepsilon_0 - \frac{j\sigma}{\omega}\right)\vec{E} = 0, \quad (2)$$

where μ_r is the relative permeability, ω is the angular frequency, ε_0 is the permittivity of vacuum, μ_0 is the permeability of vacuum, ε_r is the relative permittivity, σ is the electrical conductivity.

Then, the electromagnetic power loss *Qe* of the processing materials can be obtained from the computed electric field by the following equation [24, 25]:

$$Q_e = \frac{1}{2}\omega\varepsilon_0\varepsilon' tan\delta\left|\vec{E}\right|^2 = \frac{1}{2}\omega\varepsilon_0\varepsilon''\left|\vec{E}\right|^2, \quad (3)$$

where ε_0 is the permittivity of vacuum, ε' is the real part of the relative permittivity, ε'' is the imaginary part of the relative permittivity of the processing seeds, *tan* δ is the loss tangent of the processing materials.

For the heat transfer process, only the processed materials were taken into account in order to reduce the computation cost. The governing equation for heat transfer in solid is given as [26, 27, 28]:

$$\rho C_p \frac{\partial T}{\partial t} - k\nabla^2 T = Q = Q_e, \quad (4)$$

where ρ is the material density, *Cp* is the material heat capacity under atmospheric pressure, *T* is the temperature, *Q* is the heat source and *k* is the thermal conductivity.

2.1.4. Input Parameters and Boundary Conditions

To complete the simulation, property parameters and boundary conditions were needed. The input parameters are shown in Table 2. The thermal and dielectric properties of the maize seeds are obtained from related literature [29, 30, 31, 32].

Table 2
Summary of material properties applied in the model

	Parameter	Value
air	relative permeability μ_r	1
	relative permittivity ε_r	1
	electrical conductivity **σ** (S/m)	0
	density **ρ** (kg/m^3)	1.205
	thermal conductivity **k** (W/mK)	2.524 x10^{-2}
	heat capacity **Cp** (J/kgK)	1005
wall	relative permeability μ_r	1
	relative permittivity ε_r	1
	electrical conductivity **σ** (S/m)	5.998x10^7
maize seed	relative permeability μ_r	1
	relative permittivity ε_r	6.25-1.3·j
	electrical conductivity **σ** (S/m)	0
	density **ρ** (kg/m^3)	1250
	thermal conductivity **k** (W/mK)	0.15
	heat capacity **Cp** (J/kgK)	1700

The complex relative permittivity is defined as the processing materials to give a near-actual model, which is expressed as [33]:

$$\varepsilon_r = \varepsilon' - \varepsilon'' = \varepsilon'(1 - jtan\delta), \quad (5)$$

Other surfaces are all defined as a perfect electric conductor, which can be expressed as the equation:

$$\vec{n} \times \vec{E} = 0, \quad (6)$$

where $\vec{n}$ is the unit normal vector of the corresponding surface.

The dryer wall material was defined as the thermal insulation boundary condition. The governing equation is given as:

$$-\vec{n} \cdot \vec{q} = 0, \quad (7)$$

where $\vec{q}$ is the heat flux.

2.1.5. Simulation Process

In the simulation, the electromagnetic field distribution was first calculated in the frequency domain, and then the dissipated power was calculated. Finally, the temperature rise of the material was updated based on the heat transfer equation in the time domain. Since the electrical properties of seeds do not vary with temperature, the electromagnetic field distribution will not change and is calculated only once. The simulation time for the proposed model, for a period of 20 seconds, was about 6 hours with a workstation with two processors and a 128 Gb RAM memory.

3. Results and Discussion

The simulation results show the temperature distribution in the seed layer at the bottom of the dryer, and the distribution of the electric field in the dryer. In the hybrid dryer the seeds have reached a temperature of 30°C due to the warm air that transports them pneumatically. As a result of the action of the electromagnetic field, the temperature of the seeds increased progressively in volume, reaching a maximum temperature of 44°C during the simulation of the first 12 s of the process.

According to the experiments performed on this dryer, at a feed rate with maize seeds of 500 kg/h, and a warm air velocity of 20-25 m/s, the maximum stagnation time of the seeds in the dryer was 20 s. The seeds were discharged from the dryer periodically, every 3-4 seconds, and their temperature reached a maximum of 44°C. The simulation shows a maximum temperature in the seed layer of 44 °C after a period of 9 s and 12 s respectively (Figure 4).

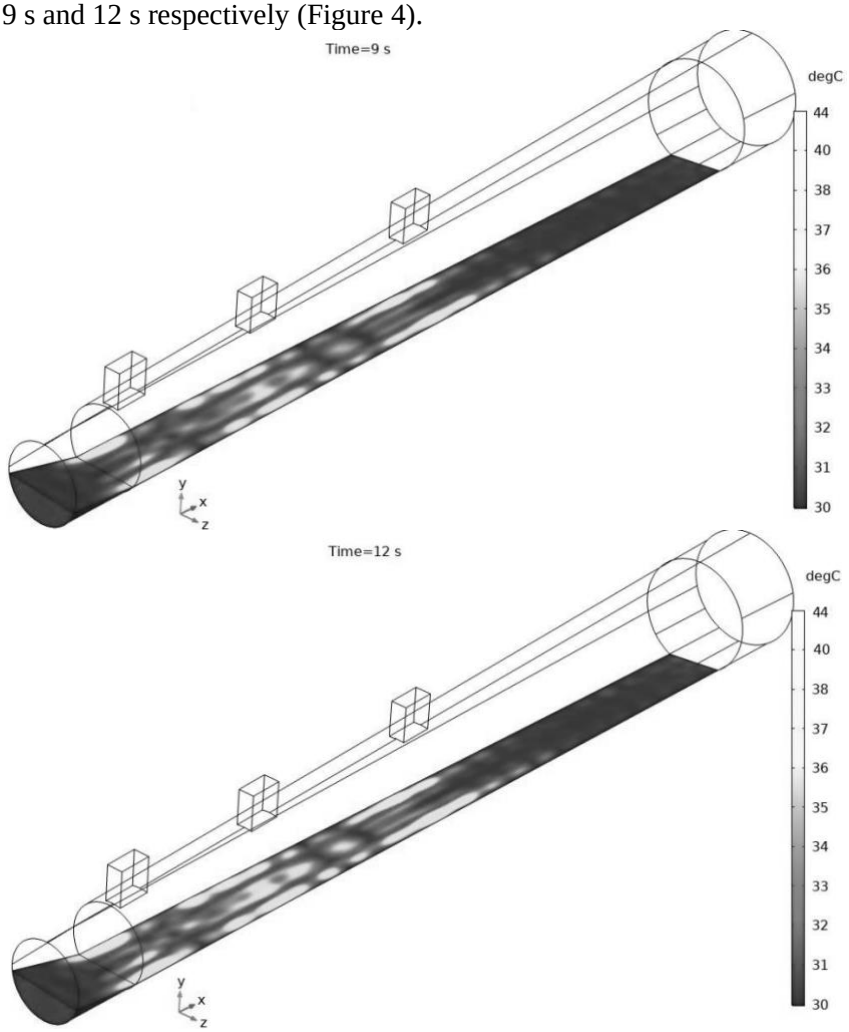

Figure 4: Temperature field [°C] in the seed layer for two periods of time (9 s, 12 s)

Due to the small size of the maize seeds compared to the size of the layer formed at the base of the dryer, virtually all seeds will heat up evenly from inside to outside, depending on the location of the remaining moisture in the grain. The lighter dried maize seeds, which do not settle to the base of the dryer, are transported to the top of the layer of the warm air at an average temperature of 44 °C. The eddy currents formed in the dryer during the pneumatic transport of the maize seeds resulted in a spiral trajectory in the first half of the dryer, with a tendency to deposit in the second half of it. The spiral movement of the seeds in the first half of the dryer made them benefit from the electromagnetic waves that have maximum power in the areas near the walls of the dryer, according to the distribution of the electric field in Figure 5.

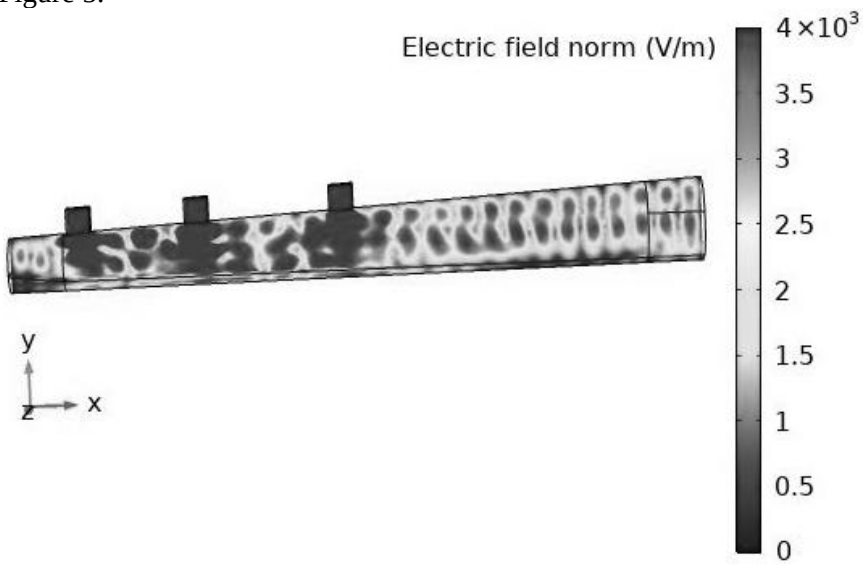

Figure 5: Distribution of the electromagnetic field inside the dryer E (V/m)

4. Conclusions

In this paper, a model was built that combines electromagnetic phenomena with heat transfer for drying cereal seeds, and a study was performed regarding the independence of the discretization grid in the field of computing for a good accuracy of the results. By simulating in the COMSOL Multiphysics software, results were obtained for the distribution of the temperature field in the maize seed layer at the base of the dryer and of the distribution of the electric field in the hybrid dryer. The results indicated that under the action of the electric field in the dryer, the maximum temperature in the seed layer was 44 °C after a period of 9-12 seconds. By losing moisture, the seeds become lighter, being transported around the top of the seed layer, and discharged from the dryer every 3-4 seconds when the feed rate of maize seed is 500 kg/h. The spiral movement of the seeds in the first half of the dryer in the regions with maximum power distribution of the electric field lead to an uniform temperature in the seed volume, thus achieving a uniform drying.

5. Acknowledgements

This work was supported by a grant of the Romanian Ministry of Education and Research, project number CNCS/CCCDI-UEFISCDI, project number PN-III-P2-2.1-PED-2019-3001, within PNCDI III, contract no. 378PED/2020. Thanks for all your support.

6. References

[1] C. D. Clary, S. J. Wang, V. E. Petrucci, Fixed and incremental levels of microwave power application on drying grapes under vacuum, J. Food Sci. 70 (5) (2005) 344–349. doi: 10.1111/j.1365-2621.2005.tb09975.x.

[2] S. Bai-Ngew, N. Therdthai, P. Dhamvithee, Characterization of microwave vacuum-dried durian chips, J. Food Eng. 104 (2011) 114–122. doi:10.1016/j.jfoodeng.2010.12.003.
[3] Z. W. Cui, C. Y. Li, C. F. Song, Y. Song, Combined microwave-vacuum and freeze-drying of carrot and apple chips, Dry. Technol. 26 (12) (2008) 1517–1523. doi: 10.1080/07373930802463960.
[4] Y. Lu, M. Zhang, H. Liu, A. S. Mujumdar, J. Sun, D. Zheng, Optimization of potato cube drying in a microwave-assisted pulsed spouted bed, Dry. Technol. 32 (2014) 960–968. doi: 10.1080/07373937.2013.877024.
[5] H. Vega-Mercado, M. M. Gongora-Nieto, G. V. Barbosa-Canovas, Advances in dehydration of foods, J. Food Eng. 49 (2001) 271–289. doi: 10.1016/S0260-8774(00)00224-7.
[6] D. G. Prabhanjan, G.S.V. Raghavan, R. G. Bosisio, Microwave drying of wheat using surface wave applicator, Powder Handling Process 5 (1993) 73–77.
[7] G. R. Askari, Z. Emam-Djomeh, S.M. Mousavi, Investigation of the effects of microwave treatment on the optical properties of apple slices during drying, Dry. Technol. 26 (11) (2008) 1362–1368. doi: 10.1080/07373930802333502.
[8] X. J. Song, M. Zhang, A. S. Mujumdar, L. P. Fan, Drying characteristics and kinetics of vacuum microwave-dried potato slices, Dry. Technol. 27 (9) (2009) 969–974. doi: 10.1080/07373930902902099.
[9] D. D. Dincov, K. A. Parrott, K. A. Pericleous, Heat and mass transfer in two-phase porous materials under intensive microwave heating, J. Food Eng. 65 (2004) 403–412. doi: 10.1016/j.jfoodeng.2004.02.011.
[10] H. Feng, J. Tang, R. P. Cavalieri, O. A. Plumb, Heat and mass transport in microwave drying of porous materials in a spouted bed, AIChE J. 47 (2001) 1499–1512. doi: https://doi.org/10.1002/aic.690470704.
[11] D. G. Prabhanjan, H. S. Ramaswamy, G. S. V. Raghavan, Microwave-assisted convective air-drying of thin layer carrots, J. Food Eng. 25 (1995) 283–293.doi:10.1016/0260-8774(94)00031-4.
[12] M. Maskan, Drying, shrinkage and rehydration characteristics of kiwi fruits during hot air and microwave drying, J. Food Eng. 48 (2001) 177–182. doi: 10.1016/S0260-8774(00)00155-2.
[13] C. Kumar, M. Karim, Microwave-convective drying of food materials: a critical review, Crit. Rev. Food Sci. Nutr. 59 (3) (2019) 379–394. doi: 10.1080/10408398.2017.1373269.
[14] H. Khan Md. Imran, W. Zachary, G. Yuantong, M.A. Karim, B. Bhandari, Modelling of simultaneous heat and mass transfer considering the spatial distribution of air velocity during intermittent microwave convective drying, International Journal of Heat and Mass Transfer, 153 (2020) 119668. doi:10.1016/j.ijheatmasstransfer.2020.119668.
[15] Z. Huacheng, G. Tushar, K. D. Ashim, H. Kama, Microwave drying of spheres: Coupled electromagnetics-multiphase transport modeling with experimentation. Part I: Model development and experimental methodology, Food and Bioproducts Processing, 96 (2016) 314–325. doi: 10.1016/j.fbp.2015.08.003.
[16] H. Zhang, A. K. Datta, Heating concentrations of microwaves in spherical and cylindrical foods Part Two: in a cavity, Food Bioprod. Process. 83 (C1) (2005) 14–24. doi: 10.1205/fbp.04047.
[17] M. Araszkiewicz, A. Koziol, A. Lupinska, M. Lupinski, IR technique for studies of microwave assisted drying, Dry. Technol. 25 (2007) 569–574. doi: 10.1080/07373930701226989.
[18] W. M. Cheng, G. S. V. Raghavan, M. Ngadi, N. Wang, Microwave power control strategies on the drying process II. Phase-controlled and cycle controlled microwave/air drying, J. Food Eng. 76 (2006)195–201. doi:10.1016/j.jfoodeng.2005.05.007.
[19] COMSOL Multiphysics, 2020. Material Library V5.6. COMSOL Multiphysics.
[20] QuickWave EM simulator, QWED s.c., Zwyciezcow 34/2, 03-938 Warsaw, Poland. URL: http://www.qwed.com.pl/.
[21] L. Perreux, A. Loupy, A. Petit, Nonthermal effects of microwaves in organic synthesis, In Microwaves in Organic Synthesis, 3rd ed., Chapter 4, 127–207, Wiley VCH Verlag GmbH & Co. KGaA: Weinheim, Germany, 2012.
[22] S. K. Pathak, F. Liu, J. Tang, Finite difference time domain (FDTD) characterization of a single mode applicator, J. Microw. Power Electromagn. Energy. 38 (2003) 37–48. doi: 10.1080/08327823.2003.11688486.

[23] J. Wang, T Hong, T Xie, F. Yang, Y. Hu, H. Zhu, Impact of filled materials on the heating uniformity and safety of microwave heating solid stack materials, Processes, 6-220 (2018) 1-13. doi:10.3390/pr6110220.
[24] S. A. Goldblith, D. I. Wang, Effect of microwaves on Escherichia coli and Bacillus subtilis. Appl. Microbiol. 15 (1967) 1371–1375. doi:10.1128/am.15.6.1371-1375.1967.
[25] K. M. Huang, Y. H. Liao, Transient power loss density of electromagnetic pulse in debye media, IEEE Trans. Microw. Theory, 63 (2015) 135–140. doi:10.1109/TMTT.2014.2374158.
[26] R. B. Pandit, S. Prasad, Finite element analysis of microwave heating of potato -Transient temperature profiles, J. Food Eng. 60 (2003) 193–202. doi: 10.1016/S0260-8774(03)00040-2.
[27] K. Pitchai, S. L. Birla, J. Subbiah, D. Jones, H. Thippareddi, Coupled electromagnetic and heat transfer model for microwave heating in domestic ovens, J. Food Eng. 112 (2012) 100–111. doi: 10.1016/j.jfoodeng.2012.03.013.
[28] K. Pitchai, J. Chen, S. Birla, R. Gonzalez, D. Jones, J. Subbiah, A microwave heat transfer model for a rotating multi-component meal in a domestic oven: development and validation, J. Food Eng. 128 (2014) 60–71. doi:10.1016/j.jfoodeng.2013.12.015.
[29] Y. Zhao, K. Huang, X. F. Chen, F. H. Wang, P.X. Chen, G. Tu, D.Y. Yang, Tempering-Drying simulation and experimental analysis of corn kernel, International Journal of Food Engineering, (2018) 1-10. doi:10.1515/ijfe-2017-0217.
[30] S. Zhang, N. Kong, Y. Zhu, Z. Zhang, C. Xu, 3D Model-based simulation analysis of energy consumption in hot air drying of corn kernels, Hindawi Publishing Corporation Mathematical Problems in Engineering, ID 579452 (2013), 1-12. doi: 10.1155/2013/579452.
[31] S. Weia, Z. Wangb, F. Wanga, W. Xiea, P. Chena, D. Yanga, Simulation and experimental studies of heat and mass transfer in corn kernel during hot air drying, Food and Bioproducts Processing, 117 (2019) 360–372. doi:10.1016/j.fbp.2019.08.006.
[32] E. Surducan, C. Neamtu, V. Surducan, Dielectric properties of *Zea mays* kernels – studies for microwave power processing applications, Processes in Isotopes and Molecules, Journal of Physics: Conference Series 182, 2009, pp. 1-4. doi:10.1088/1742-6596/182/1/012017.
[33] C. J. F. Böttcher, O.C. van Belle, P. Bordewijk, A. Rip, D.D. Yue, Theory of electric polarization. J. Electrochem. Soc. 121-6 (1974) 211Ca. doi: 10.1149/1.2402382.